

Computational study of gaseous detonation diffraction and re-initiation by small obstacle induced perturbations

Xueqiang Yuan^{1,2†}, Xiaocheng Mi³, Jin Zhou¹ and Hoi Dick Ng²

¹ Science and Technology on Scramjet Laboratory, National University of Defense Technology, Changsha, 410073, China

² Department of Mechanical, Industrial and Aerospace Engineering, Concordia University, Montreal, Canada H3G 1M8

³ Department of Physics, Cavendish Laboratory, University of Cambridge, CB3 0HE, UK

1 Introduction

Detonation diffraction in gases out of a confined tube into an unconfined area has long been a classical problem to understand the failure and initiation mechanism of a self-sustained detonation wave [1, 2]. For an unstable detonation in common gaseous mixtures, i.e., a propagating detonation front with irregular cellular pattern, it has been long suggested that the cellular instabilities play a prominent role in the outcome of the detonation diffraction [3]. Experimental evidences by Mehrjoo et al. [4, 5] have shown that by generating artificially flow perturbations using small obstacles or by damping transverse waves using porous media at the tube exit, they promote or suppress transmission of the diffracting detonation wave, respectively. Our recent study using high-speed schlieren flow visualization [6] shows that for a successful transmission of the diffracting detonation wave, a sufficient degree of cellular instability is needed in the quasi-steady, weakly decoupled curved reaction-shock complex persisting away from the expansion cone to subsequently generate an explosion bubble and re-initiation. To elucidate their importance on the re-initiation, the cellular instabilities at the diffracted front are further stimulated by inserting a small obstacle to promote the generation of transverse waves and a re-initiation kernel. The use of the small obstacle can also act as a probe to identify the flow region where explosion bubble can possible form for the onset of re-initiation.

In this work, numerical simulations are performed to further investigate the detonation diffraction process and the role of transverse cellular instability by generating small obstacle induced perturbations in the sub-critical regime to promote the re-initiation. The simulations are carried out by solving the two-dimensional reactive Euler equations with a two-step induction-reaction kinetic model. The present numerical results determine the locations of the small obstacle where the induced effects can induce the re-initiation of the diffracted detonation wave, and the mechanism of the promoting effect by the obstacle in the re-initiation process was examined.

[†]Correspondence to: yxq_nudt@hotmail.com

2 Computational Setup

Neglecting the viscous and diffusion, the governing equations for the detonation flow dynamics are simplified into the ideal reactive Euler equations. A two-step induction-reaction kinetic model described in [7] and used in a number of previous studies, e.g., [8-9] is employed. All the flow variables have been made dimensionless by reference to the uniform unburned state ahead of the detonation front and the pre-exponential factor k_I of the induction step is chosen to define the spatial and temporal scales, so the induction length is unit, i.e., $\Delta_I = 1$. The solutions to the governing equation system are obtained numerically using a 2nd order MUSCL-Hancock scheme with a HLLC Riemann solver [10, 11], with a CFL number of 0.90. To accelerate the simulation run-time, the entire flow solver was implemented using NVIDIA CUDA programming language (NVIDIA Corp.) [11-13] and run on a NVIDIA Tesla K40 graphics processing unit (GPU). In this work, the default resolution considered is 16 pts per induction zone length Δ_I . The dimensionless thermodynamic parameters of the combustible mixture are $Q/RT_o = 21.365$, $\gamma = 1.32$, $\varepsilon_I = 5.414$, $\varepsilon_R = 1.0$, $k_I = 1.0022$, $k_R = 4.0$, $T_s/T_o = 5.0373$ and $M_{CJ} = 5.0984$. These properties corresponds approximately to a stoichiometric hydrogen/oxygen mixture at 20 kPa and 300 K and in which an unstable detonation wave with irregular cellular pattern would form.

The computational domain is shown in Fig. 1. It had a symmetric upper boundary and hence, only half of the diffraction flow field was simulated. The width of the horizontal tube was set and determined *a priori* to obtain a detonation wave under the sub-critical condition according to the combustible mixture, and the length of the domain is made sufficient enough to observe the entire diffraction and re-initiation process. A rectangular obstacle with dimensionless sizes of 20×5 was preset in the open area. The horizontal and vertical distances of the obstacle position, d_h and d_v from the upper right corner of the obstacle to the expansion corner are varied. To initialize the computation, a self-sustained cellular detonation under the specified initial conditions was first achieved and then imposed near the exit of the horizontal tube. The cellular structure of the initial detonation wave as well as the diffraction process without obstacle is presented by the numerical soot foil in Fig. 2. It can be seen that the cellular patterns vanished when the detonation wave propagates into the open area indicating a sub-critical regime.

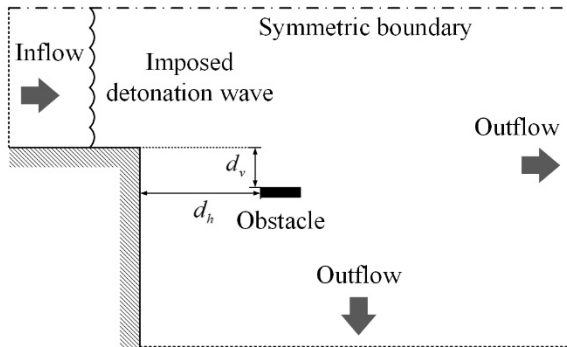


Figure 1. Schematic of the computational domain

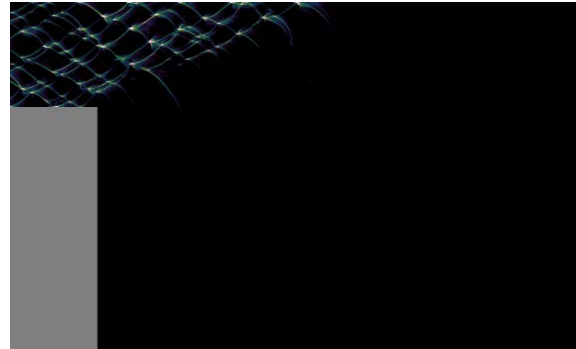


Figure 2. Numerical soot foil for the detonation diffraction under sub-critical condition with no imposed obstacle

3 Results and Discussion

The density and pressure contours in Fig. 3 show a typical re-initiation process induced by the rectangular obstacle in the open area. The obstacle position is $d_h = 500$ and $d_v = 40$. Since the mixture condition is sub-critical, the central core of the wave front at the inner side can still sustain the detonation cellular structure when the detonation wave propagates into the open area, whereas the outer side part

decouples immediately by the diffraction effect, and the cellular structure with transverse waves begin to vanish, as displayed in Fig. 3(a). When the decoupled wave front reaches the edge of the imposed small obstacle, the oblique collision between the wave front and the obstacle induces an unsteady reflection structure on the surface of the obstacle, which enhances the pressure and temperature behind the reflected wave, as shown in Fig. 3(b). Although the increased pressure and temperature zone ignites the unburned mixture in the decoupled region when the reflection triple point separates from the obstacle, shortening the distance between the combustion front and the shock wave, the energy is not enough to generate local explosion, and the wave front is still decoupled, as Fig. 3(c) shows. Simultaneously, a detonation triple-point with a transverse wave sweeps down along the diffracted wave front, colliding with the reflection triple-point which propagates upward. This collision raises the energy behind the wave front again, leading to a local explosion and generating an explosion bubble, as illustrated in Fig. 3(d). Originated from the explosion bubble, the combustion front and the shock wave front couple together with new transverse wave on it, indicating a local detonation wave structure is formed. This local detonation wave will spread towards both sides and the re-initiation will be established. Figure 4 presents the corresponding numerical soot foil. It can be found that the diffracted detonation wave is re-initiated successfully with multiple detonation cell structures formed in the end. Two bright regions, A and B, indicate the increase of energy, which corresponds to the reflection of wave front on the obstacle surface and the collision between the triple-points of detonation and reflection, respectively. To this end, the re-initiation mechanism is basically clarified that it is the aforementioned two processes that increase the energy behind the decoupled wave front, ignite mixture in the decoupled area and induce local explosion to generate an explosion bubble and finally realize the re-initiation on the entire wave front.

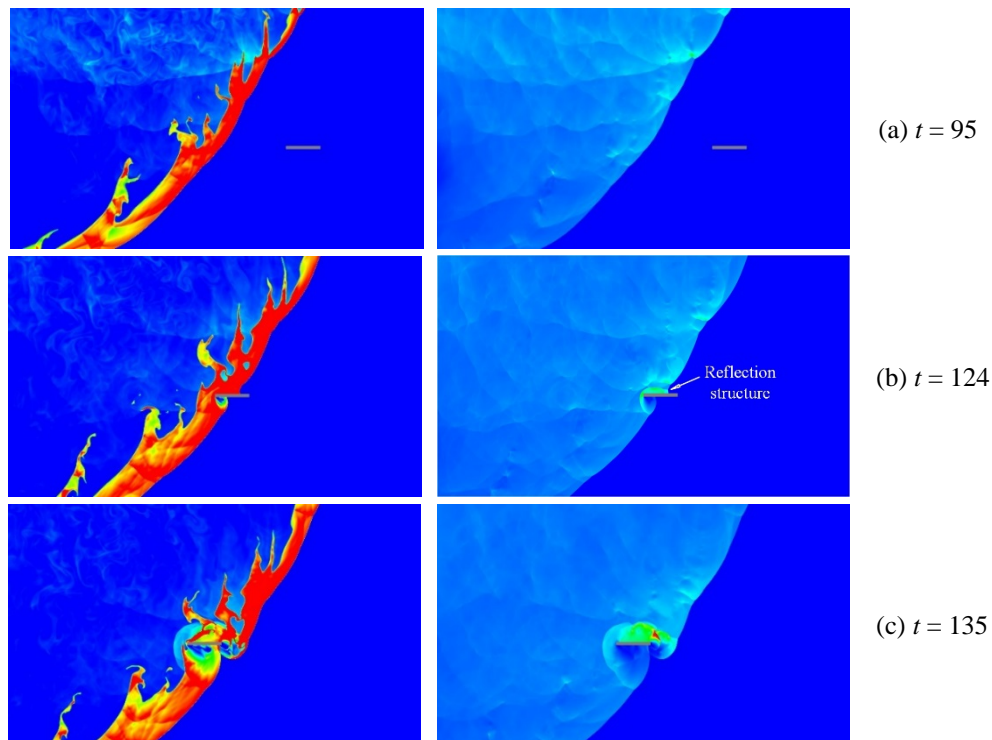


Figure 3. (continued)

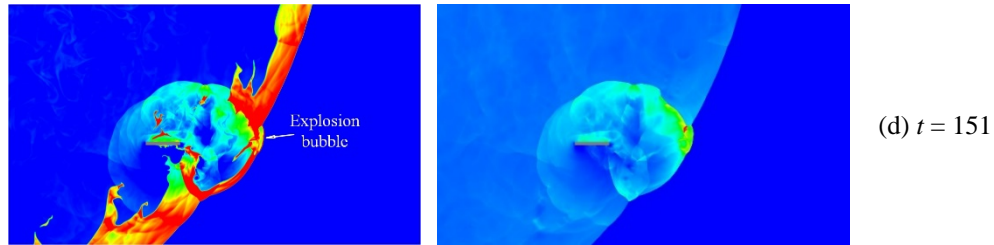


Figure 3. Contours of density and pressure presenting re-initiation process induced by obstacle

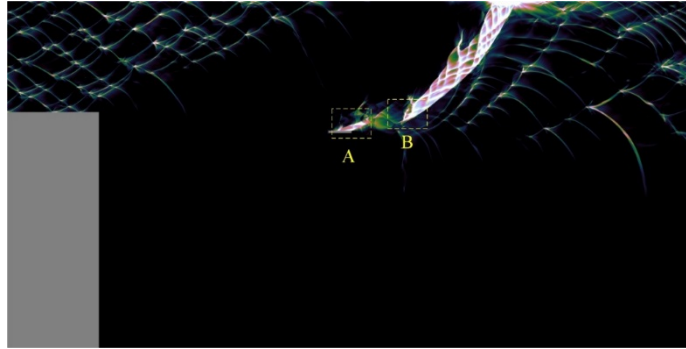


Figure 4. Numerical soot foil for successful re-initiation induced by obstacle

However, a further analysis indicates that not all the cases which experience the two processes can re-initiate the detonation. In fact, to re-initiate the detonation, an additional condition should also be satisfied, that is when the reflection structure is formed on the obstacle, a detonation triple point should just propagate to the surface of the obstacle. To express this condition clearly, the reflection process for a failed re-initiation case is shown in Fig. 5, corresponding to the obstacle position of $d_h = 450$ and $d_v = 40$. As a comparison, the same process for the successful case mentioned above is also presented. From Figs. 5(a) and (b), it can be found that the reflection structures are formed in both cases, the pressure ratio p/p_0 behind the reflected wave is about 30. The difference is that in the successful case, there is a detonation triple-point with a transverse wave just reaches the obstacle, hence a series of collisions and reflections related to the reflection triple-point, the detonation triple-point and the obstacle surface happen in a very short time, which raises the pressure ratio p/p_0 to over 120, as seen in Fig. 5(d). Such high energy can sustain the combustion behind the decoupled wave front effectively until the local explosion is induced. While in the failed case, no coherent detonation triple-point propagates to the obstacle at this time, and the p/p_0 steadies at about 30 in the whole reflection process, as seen in Fig. 5(c). Hence, although the triple-points of detonation and reflection collide afterwards, the energy is still unable to realize the re-initiation. This result also implies that the position and size of the obstacle are important elements for the detonation re-initiation.

To investigate the effect of the obstacle position on the re-initiation of the diffracted detonation wave, a series of simulations with the same initial and mixture conditions were conducted with various obstacle positions. The parameter d_h is varied from 50 to 700 with an increment of 50, and d_v is varied from -120 to 120 with an increment of 20. The re-initiation result for each case was record and displayed schematically in Fig. 6, combined with the numerical soot foil with no obstacle. It can be observed that for all the cases, just a few of the positions can re-initiate the detonation successfully, and most of the successful cases distribute in the area of $100 \geq d_v \geq 40$, the reason is that the area of $d_v < -40$ is close to or even at the inner side of the expansion wave front, where the detonation wave front does not decouple completely, so there is no enough unburned mixture in the decoupled region to ignite and induce local explosion, whereas in the area of $d_v > 100$, the detonation wave front has been fully decoupled with barely no detonation transverse

wave on it, which is impossible to obtain enough energy to re-initiate the detonation. In addition, in all the successful cases, there must be at least one long trajectory of detonation triple point at the right side of the obstacles, this rule corresponds to the re-initiation mechanism described before that in order to enhance energy to realize local explosion, the reflection triple point should collide with a detonation triple point when it separates from the obstacle. This rule also implies that the detonation cannot be re-initiated if the obstacle is set at the right side of the last detonation triple-point trajectory (including on the trajectory). Moreover, the results show another significant rule that the obstacle regions in the successful cases always intersect with the trajectories of detonation triple points, which corresponds to the additional condition of re-initiation described previously. The intersection indicates that the detonation triple point surely will reach the surface of the obstacle at a certain time, causing collisions and reflections among the reflection triple-point and the obstacle surface, and raising the energy behind reflected wave greatly. It should be noted that there is also requirement for the energy of the detonation triple point to realize re-initiation. By extracting the pressure peak at the intersection point for the successful cases, the critical pressure ratio for the detonation triple point is about 16. On the other hand, it is found that almost all the cases with no trajectory intersect the obstacle region are failed, which means that the interaction among cellular detonation and reflection triple point as well as the obstacle seems necessary for the detonation re-initiation. The analysis above provides guidance for the further study of the obstacle size effect and theoretical study for confirming the successful re-initiation area.

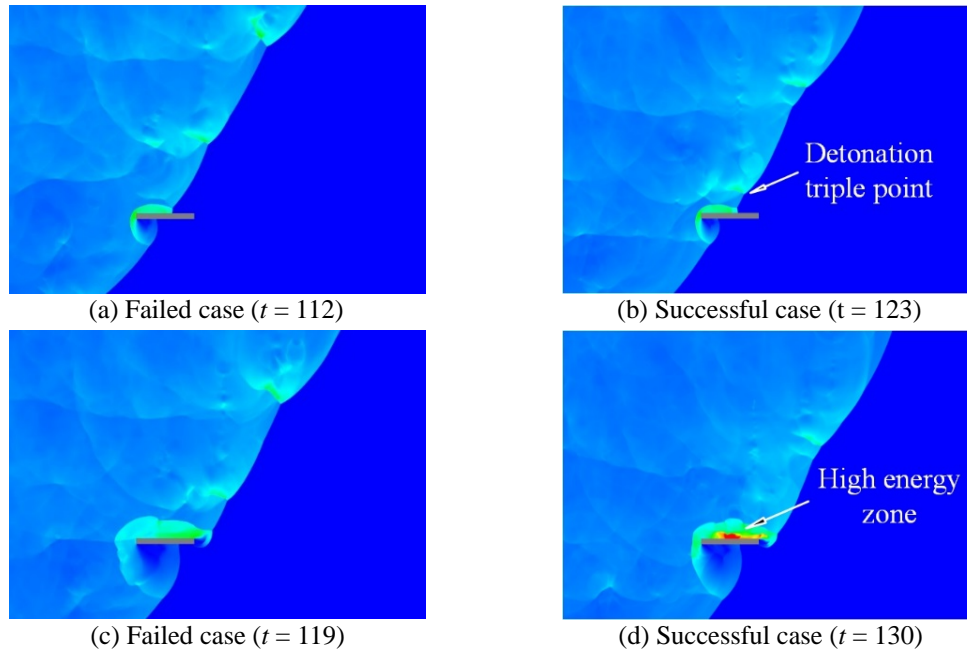


Figure 5. Contours of pressure showing the reflection process of both the failed and successful cases.

4 Concluding Remarks

In summary, this work investigates numerically the effect of small obstacle induced perturbations on the re-initiation of a diffracted detonation wave and highlighted the importance of cellular instability. For successful re-initiation, sufficient cellular instabilities and triple points (either survived naturally or induced artificially) must be sustained to cause the explosion bubble for the onset of re-initiation. By using the small obstacle as a probe, the present numerical simulations also pinpoint the location and illustrate the mechanism for the successful transmission of a detonation from a confined space to an open area.

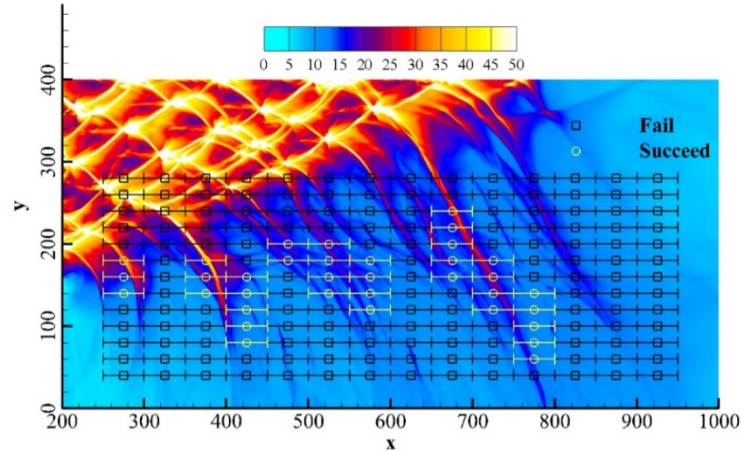


Figure 6. Re-initiation result for each case combined with numerical soot foil with no obstacle.

Acknowledgement

This work is supported by the Natural Sciences and Engineering Research Council of Canada NSERC (No. RGPIN-2017-06698).

References

- [1] Lee JHS. (2008) *Detonation Phenomenon*. Cambridge University Press, NY.
- [2] Pintgen F, Shepherd JE. (2009) Detonation diffraction in gases. *Combust. Flame* 156(3): 665.
- [3] Lee JHS. (1996) On the critical tube diameter. In: Bowen, J. (ed.) *Dynamics of Exothermicity*, pp. 321 Gordon and Breach, Amsterdam.
- [4] Mehrjoo N, Zhang B, Portaro R, Ng HD, Lee JHS. (2014) Response of critical tube diameter phenomenon to small perturbations for gaseous detonations. *Shock Waves* 24(2): 219.
- [5] Mehrjoo N, Gao Y, Kiyanda CB, Ng HD, Lee JHS. (2015) Effects of porous walled tubes on detonation transmission into unconfined space. *Proc. Combust. Inst.* 35(2): 1981.
- [6] Xu H, Mi XC, Kiyanda CB, Ng HD, Lee JHS, Yao C. (2019) The role of cellular instability on the critical tube diameter problem for unstable gaseous detonations. *Proc. Combust. Inst* 37(3): 3545-3553.
- [7] Ng HD, Radulescu MI, Higgins AJ, Nikiforakis N, Lee, JHS. (2005) Numerical investigation of the instability for one-dimensional Chapman-Jouguet detonations with chain-branching kinetics. *Combust. Theory Modell.* 9: 385.
- [8] Zhang Y, Teng HH, Ng HD, Wen C. (2018) Transition between different initiation structures of wedge-induced oblique detonations. *AIAA J.* 56(10): 4016.
- [9] Yuan XQ, Zhou J, Mi XC, Ng HD. (2019) Numerical study of cellular detonation wave reflection over a cylindrical concave wedge. *Combust. Flame* 202: 179-194.
- [10] Toro EF. (2009) *Riemann Solvers and Numerical Methods for Fluid Dynamics*, Springer-Verlag, Berlin
- [11] Kiyanda CB, Morgan GH, Nikiforakis N, Ng HD. (2015) High resolution GPU-based flow simulation of the gaseous methane-oxygen detonation structure. *J. Visualization* 18(2): 273.
- [12] Mi XC, Higgins AH, Ng HD, Kiyanda CB, Nikiforakis N. (2017) Propagation of gaseous detonation waves in a spatially inhomogeneous reactive medium. *Phys. Rev. Fluids* 2: 053201.
- [13] Mi XC, Higgins AH, Kiyanda CB, Ng HD, Nikiforakis N. (2018) Effect of spatial inhomogeneities on detonation propagation with yielding confinement. *Shock Waves* 28(5): 993-1009.